29 May 2010, 8:00 am - 9:30 am

Experimental and Numerical Study of Topographic Site Effect on a Hill Near Tehran

Mohammad Khandan Bakavoli
International Institute of Earthquake Engineering and Seismology, Iran

Ebrahim Haghshenas
International Institute of Earthquake Engineering and Seismology, Iran


Fifth International Conference on
Recent Advances in Geotechnical Earthquake Engineering and Soil Dynamics
and Symposium in Honor of Professor I.M. Idriss
May 24-29, 2010 • San Diego, California

EXPERIMENTAL AND NUMERICAL STUDY OF TOPOGRAPHIC SITE EFFECT ON A HILL NEAR TEHRAN

Mohammad Khandan Bakavoli
International Institute of Earthquake Engineering and Seismology
Tehran, Iran.

Ebrahim Haghshenas
International Institute of Earthquake Engineering and Seismology
Tehran, Iran.

ABSTRACT

This paper compares the experimental study of seismic response of a hill site near Tehran and numerical modeling of the test site using a hybrid finite-boundary element code named HYBRID. Both longitudinal and transversal profiles of the hill have been instrumented using Guralp CMG-6TD seismological stations and some hours of ambient noise were recorded. The H/V ratios for each station were calculated and the amplification patterns and corresponding frequencies of each station have been extracted. Then the two profiles has been modeled numerically and excited by vertically incident SV ricker waves with different fundamental frequencies. The medium is assumed to have a linear elastic constitutive behavior. All calculations are executed in time-domain using direct boundary element method. The amplification patterns, both in time domain and frequency domain, have been determined. The similarities and discrepancies between the experimental and numerical methods have been discussed. It was shown that using microtremor would not be an efficient way for estimating the topographic site effect and may not be applied for microzonation studies of the elevated areas.

INTRODUCTION

Variation of seismic ground motion due to the effect of topography features have been approved by the observed variant damage on these features during large earthquakes. Many cases in this regard are reported in Celebi 1991 (Coalinga earthquake 1983), Celebi 1987 (Chili earthquake 1985), Ashford and Sitar (Northridge earthquake 1994) and recent earthquakes in Greece (Athanasopoulos et al., 1999). Besides, very high accelerations recorded at the Pacoima Dam (1.25g) during the 1971 San Fernando earthquake (Trifunac and Hudson, 1971) and at the Tarzana hill (1.78g) during the 1994 Northridge earthquake (Spudich et al., 1996) have been partly attributed to topographic effects. Recent developments in numerical modeling of wave propagation across hills help to explain topographic effects, but there are sometimes discrepancies between experimental and numerical results. Review of the published works show that, generally there is an amplification of the ground motion at the top of the hill and a de-amplification at the base. This amplification is frequency dependent and has a maximum value at a frequency called the resonance frequency of the hill; this effect is more important on the horizontal than on the vertical components and it is larger along the direction of motion perpendicular to the hill. Iran is a part of the well known seismic belt of the world and is considered as an earthquake-prone region with a high seismic hazard level. In the recent years the developments of the cities on the areas with topographic irregularities become an important problem from the view point of earthquake hazard and risk. Some researches on the numerical and experimental studies of the effect of topography have been started. The preliminary results of an experiment, carried out near Tehran, the capital are introduced in the presented article.

SITE DESCRIPTION

The studied site is located in south east of Tehran, in the eastern margin of Shahr-e-Rey. Figure 1 shows the location of the studied hill on the satellite image of the Tehran region. The hill is a continuation of the Bibi Shahrbanoo mountain toward the inner part of the city. This is a mound consisted from the dolomite and limestone belonging to the Triassic and Cretaceous geological periods. This site was selected due to its homogeneity and absent of the soft soil layers. In this way we can assumed that the variation of seismic motion is only due to topographic effect and not to the local week layers.

EQUIPMENT USED

The broadband Guralp CMG-6TD, three components digital seismometer were used in microtremor measurements. Each sensor is sensitive to ground vibration over a wide frequencies ranging 0.033-50 Hz. The sensors can be supplied with a response which is flat to velocity from 100 Hz to any of 1 Hz, 0.1 Hz, 0.033 Hz and 0.016 Hz. The ultra-light, quick and easy, one person installation makes it suitable for field work.

FIELD EXPERIMENT

The topographic map of the hill is shown in fig. 1. As in the meanwhile, just five seismometers were available, the microtremor recording has been carried out in two days, one for longitudinal profile and second day for transverse profile. These five seismic stations were installed across the hill in each direction. Two stations were located on each side of the foothill. Two stations were installed along the slope and one at the top of the hill.

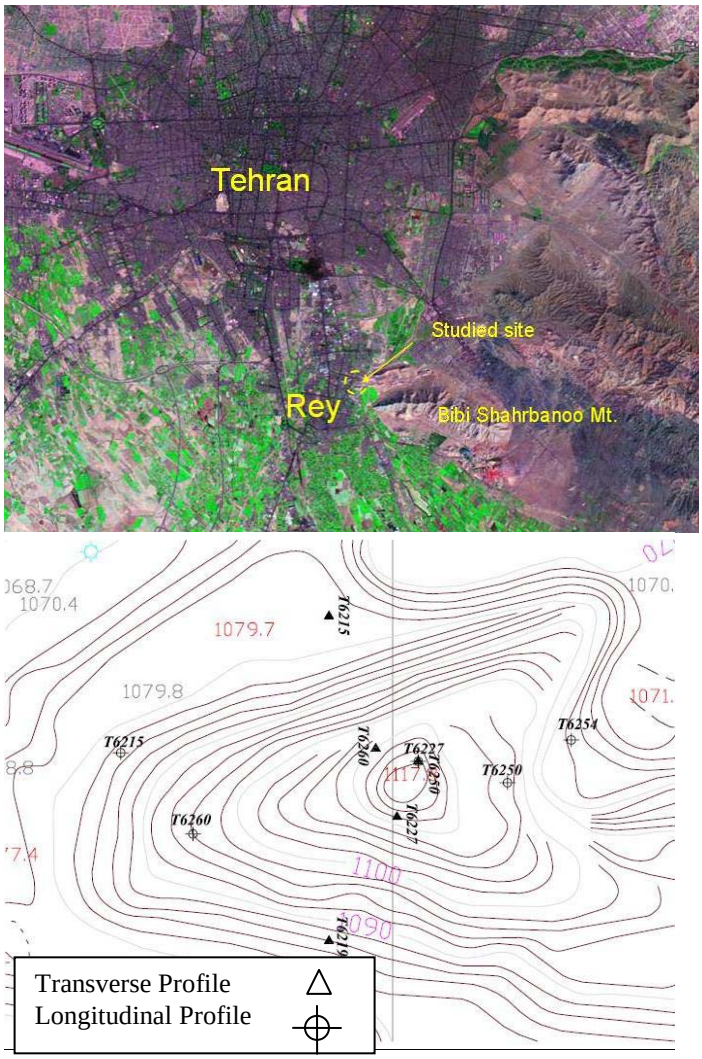

Fig. 1. Location of the studied hill(above) and the topographic map of the hill.

DATA PROCESSING

The first method used here to determine site effects is horizontal to vertical spectral ratio calculated on the ambient noise also called Nakamura's method or HVNR (Nakamura, 1989). All the spectral ratios were calculated using the Geopsy software provided by the European SESAME consortium applying the following procedure. The continuously recorded data were split into 30 minutes microtremor records. The stationary noise windows of 20 to 30 minutes were selected by the anti-triggering algorithm incorporated in the software with a 5% window overlapping. The Konno-Ohmachi smoothing function has been used to avoid spurious peaks or sharp troughs in the spectra. To minimize the border effects due to the windowing of the Fourier spectra, 5% cosine taper has been used.

In addition to the H/V technique, in order to confirm the results, the other signal processing techniques normally used in the system identification studies (Ex. Davoodi et al. 2008) were applied. This technique is based on comparing the different spectra such as fast Fourier spectra, power spectral density (PSD), cross power spectra (CPS), and also coherency spectra (CS) between two points and also phase spectra,. The records have been band pass filtered and detrended before calculating the above spectra. A peak on PSD curves at any response point either represents a resonance frequency associated with the mode of vibration of the structure or corresponds to a peak in the excitation spectrum. To distinguish the spectral peaks representing the modes of vibration from those corresponding to peaks in the input spectrum, the amplitude and phase of CPS may be used. That is, all points of the hill in a lightly damped mode of vibration are in phase or 180° out-of-phase with each other, depending on the shape of the normal mode. The phase relationships between two response measurement points are obtained from the cross correlation phase spectrum (CCPS).

RESULTS OF MICROTREMOR MEASUREMENTS (H/V)

Many spectral ratios were computed, they cannot all be displayed here. The average curves for each station in both directions, transverse and longitudinal, have been plotted. The extracted average curves obtained for ten 30 minutes microtremor recordings for all stations in the longitudinal profile and eight 30 minutes recordings for the transverse profile (Fig. 2 and 3).

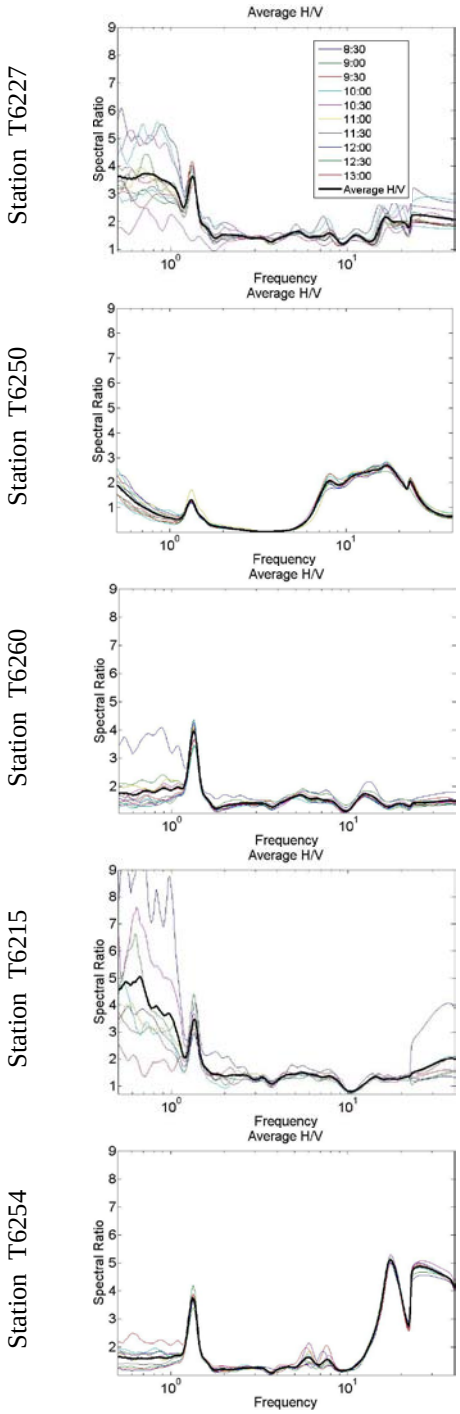

Fig. 2. The H/V curves for stations along the longitudinal profile.

Both in transverse and longitudinal sections, a very obvious and narrow peak can be observed at frequency of 1.3 Hz, having a similar amplification value for all the stations, except station T6250. This similarity and also comprehensive studies of Haghshenas 2005 has been revealed that there is an industrial source corresponding to this frequency. At other frequencies, in longitudinal profile, there would not be any systematic amplification. However, in transverse profile, in the amplification curves correspond to the stations located along the slope and on the top, show an amplification around frequency near 10 Hz. On the contrary, a trough could be recognized, around 10 Hz, on the amplification curves related to the stations located at the foothill. This may correspond to topographic site effect which causes amplification and de-amplification on the irregularity.

As the studied irregularity is relatively small, the source of the recorded microtremor assumed to be the same, so the spectral ratio between horizontal components of the stations located along the slope to the station installed at the foothill would be another choice to study the behavior of the hill.

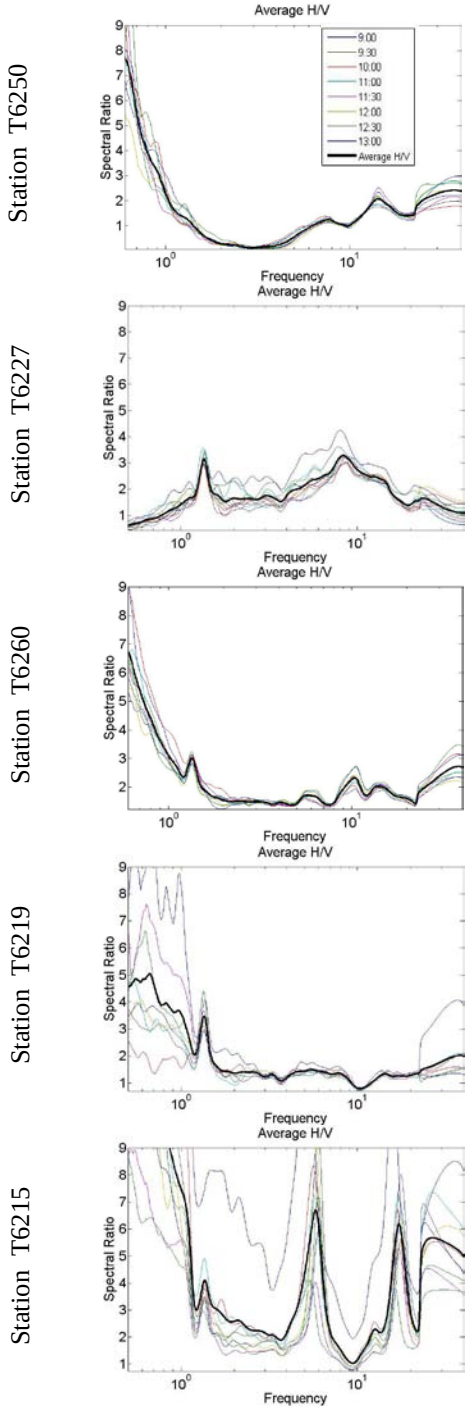

Fig. 3. The H/V curves for stations along the transverse profile.

RESULTS OF CLASSICAL SIGNAL PROCESSING TECHNIQUE (4-SPECTRA METHOD)

The 4-spectra method is an easy and straight forward method to process stationary signals (Jafari and Davoodi, 2006). For all stations, in both directions, the four spectra for each two stations have been produced.

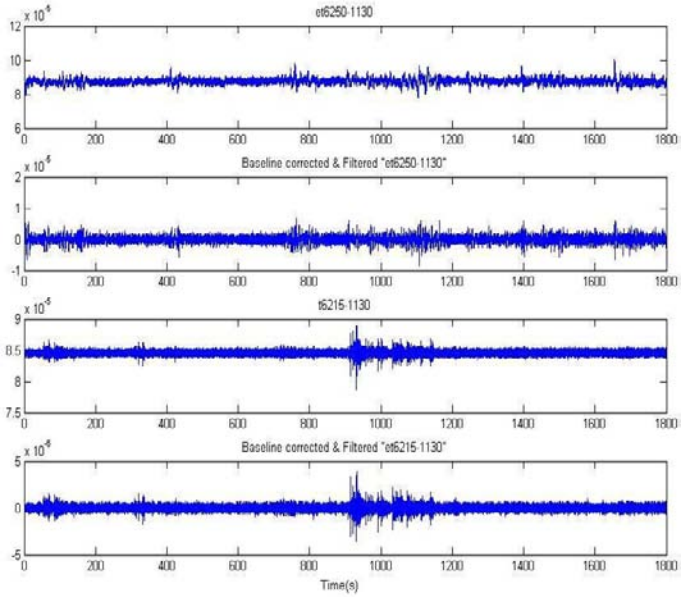

Fig. 4. Raw and filtered signals of stations T6250 and T6215.

By comparing the obtained results in all stations and using the mentioned technique, the frequencies of the hill could be identified. For instance, the raw and filtered signals of stations T6250 and T6215, located at the top and the base of the hill

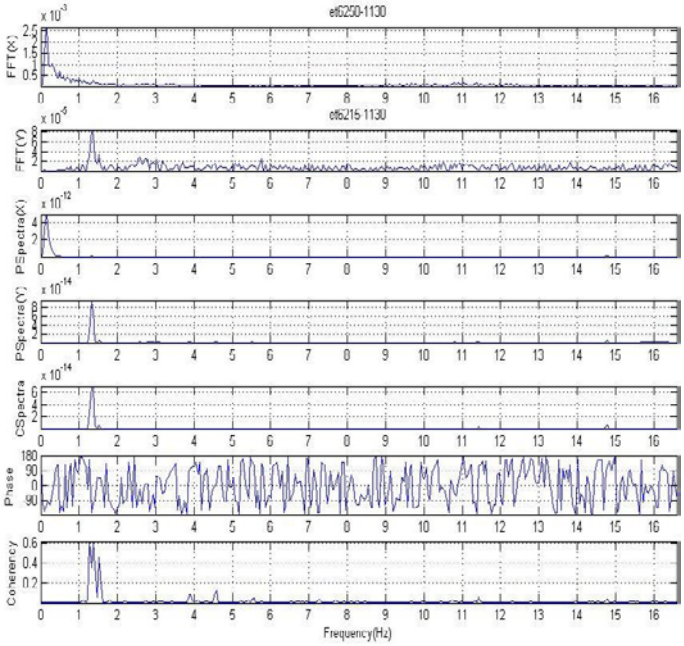

Fig. 5. Raw and filtered signals of stations T6250 and T6215.

respectively, has been shown in fig. 4. Figure 5, shows the four spectra calculated for these two stations. By comparing the spectra, the frequency of 1.3 Hz would be the only obvious candidate for the structure. All the spectra have peak in this

frequency and also the phase angle is between 0° and 90° which shows that the motion of the points would be in phase.

NUMERICAL MODELING

The numerical modeling of the longitudinal and transverse profile has been carried out using the boundary element based code named HYBRID. This study performed using the following well-known transient boundary integral equation governing the dynamic equilibrium of isotropic elastic media (Kamalian et al 2006).

$$c_{ij}(\xi)\cdot u_i(\xi,t)=\int (G_{ij} * t_i(x,t)-F_{ij} * u_i(x,t))d\Gamma \quad (1)$$

Where u_i denotes the displacement vector and t_i represents the traction at the boundary. G_{ij} and F_{ij} are the transient displacement and traction kernels respectively, and represent the displacements and tractions at a point x at the time t due to a unit point force applied at ζ and at the preceding time τ. The terms $G_{ij} * t_i$ and $F_{ij} * u_i$ are the Riemann convolution integrals and c_{ij} denotes the well-known discontinuity term resulting from the singularity of the F_{ij} kernel.

The layout of the model (longitudinal profile) has been shown in fig. 6 and 7. The model consisted of 439 point at the boundary and 219 quadratic boundary elements and 319 enclosing elements. The hills were subjected to vertically propagating incident SV wave of the Ricker type;

$$f(t)=\left[1-2\cdot(\pi\cdot f_p(t-t_0))^2\right]\exp^{-(\pi\cdot f_p\cdot(t-t_0))^2} \quad (2)$$

In which f_p and t_0 denote the predominant frequency and appropriate time shift, respectively.

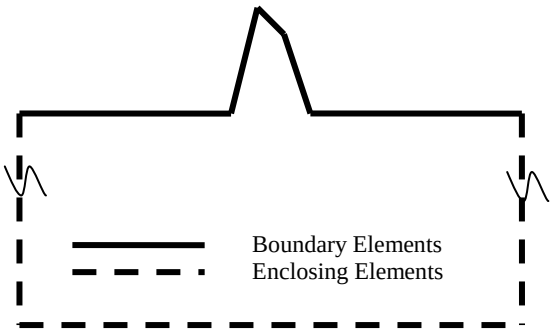

Fig 6. Raw Schematic geometry and discretization of the hill.

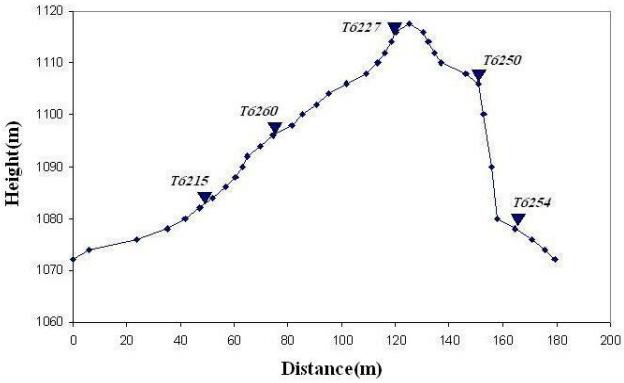

Fig. 7. The longitudinal profile with the stations located at the hill.

The material properties of the model have been described in table 1.

Table 1. Material property of the model.

Bulk Modulus	3680000 KN/M^2	Poisson Ratio	0.38
Elasticity Modulus	5080000 KN/M^2	Time step	100
Unit weight	24.5 KN/M^3	Shear Velocity	737.5 m/s

The model is excited by an SV Ricker waves with different predominant frequencies ranging from 2 Hz to 10 Hz.

GENERAL AMPLIFICATION PATTERN

Fig. 8 and 9 shows the time-domain response of the studied hill which has been subjected to a vertically propagating incident SV Ricker wave with a predominant frequencies of 3Hz and 10Hz, respectively.

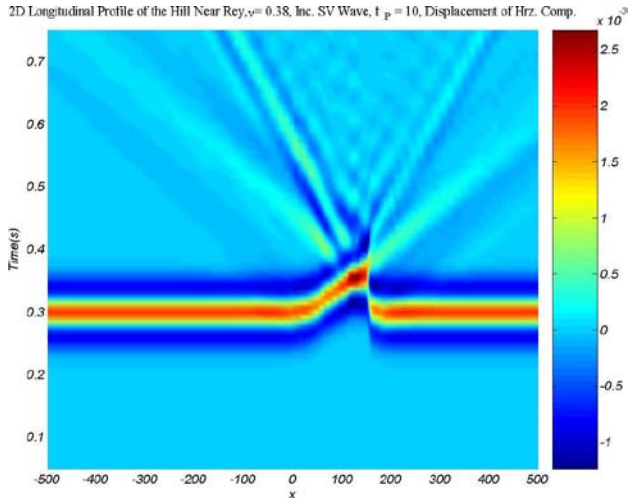

Fig. 8. Incidence of a vertically propagating SV wave (freq. 10 HZ). Synthetic seismogram for surface receivers between x = −500 and x = 500 at surface of the hill.

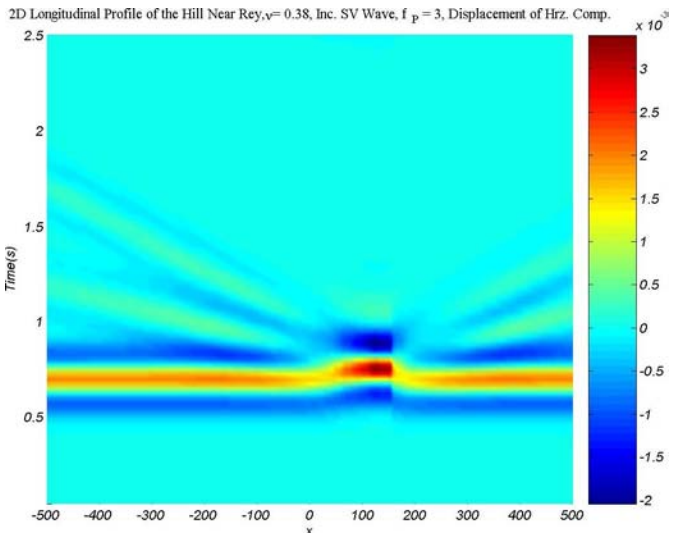

Fig. 9. Incidence of a vertically propagating SV wave (freq. 10 HZ). Synthetic seismogram for surface receivers between x = −500 and x = 500 at surface of the hill.

Besides, the amplification pattern of the hill, the horizontal components of the motion, consists of sequential amplification and deamplification has been shown in fig. 10 and 11. Considering amplification pattern of the hill, at any point on the ground surface, irrespective of being on the hill or on the half-plane, the total motion differs from the free field motion (twice the incident motion). The motion may be amplified or de-amplified, depending on the predominant frequency of the incident wave.

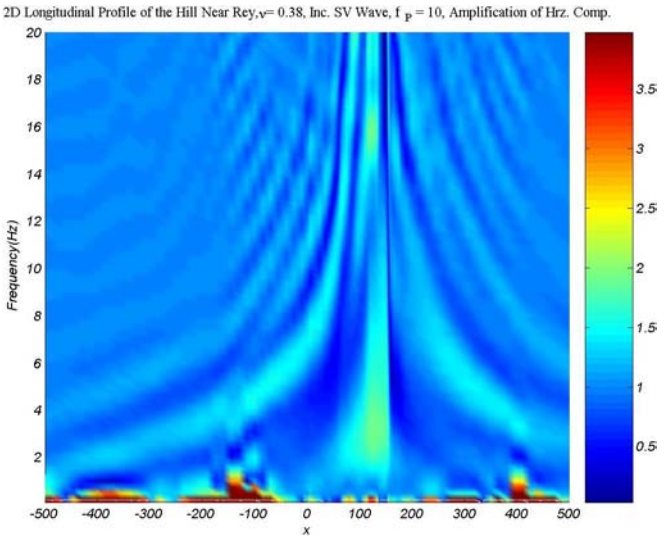

Fig. 10. Incidence of a vertically propagating SV wave (freq. 10Hz). Amplification pattern of horizontal component of motion for surface receivers between x = −500 and x = 500 at surface of the hill.

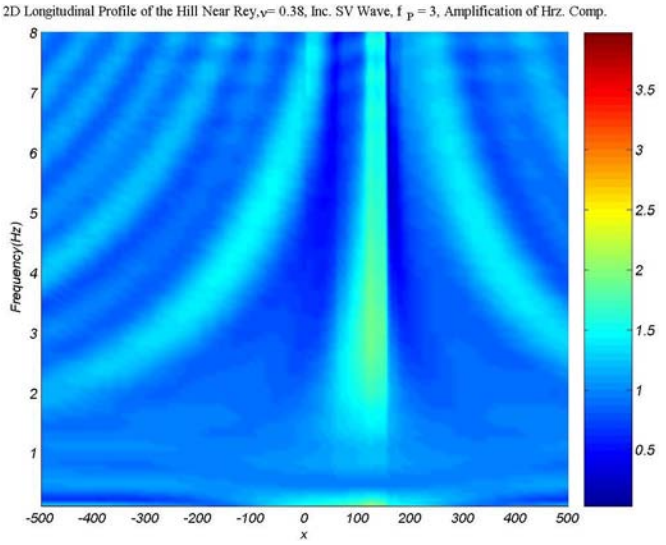

Fig. 11. Incidence of a vertically propagating SV wave (freq. 10Hz). Amplification pattern of horizontal component of motion for surface receivers between x = −500 and x = 500 at surface of the hill.

The amplification curve of the hill finds its maximum at the crest and decays towards the bases. If the incident wave has a predominant frequency smaller than the frequency of the hill, decreasing the frequency of the wave reduces the effect of the hill on the ground motion. The amplification ratio of the crest has been shown in fig. 12 and 13 for two groups of incident waves, incident Ricker SV wave with predominant frequency of 2-4 Hz and the other with predominant frequency of 6-10 Hz, respectively.

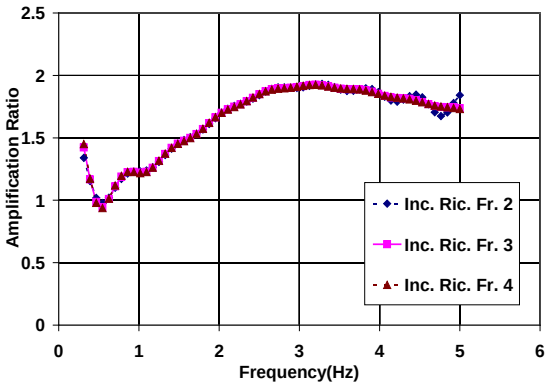

Fig. 12. Incidence of a vertically propagating SV wave (freq. 2-4Hz). Amplification of the crest of the hill (longitudinal profile).

Moreover, the amplification pattern of the hill, the vertical components of the motion, consists of sequential amplification and deamplification has been shown in fig. 14 and 15. As it can be seen there is a very slight amplification and deamplification on vertical component of the motion.

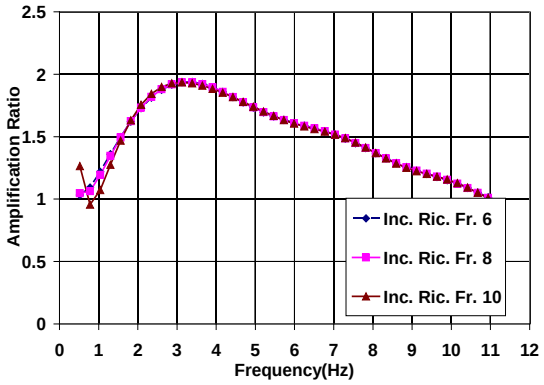

Fig. 13. Incidence of a vertically propagating SV wave (freq. 6-10Hz). Amplification of the crest of the hill (longitudinal profile).

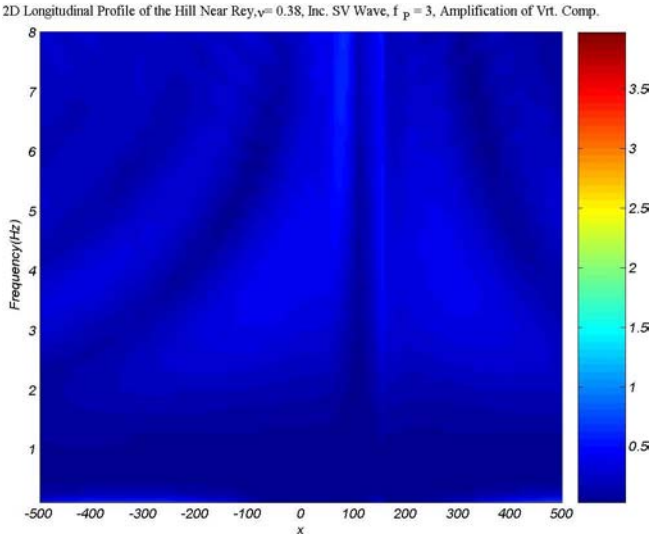

Fig. 14. Incidence of a vertically propagating SV wave (freq. 3Hz). Amplification pattern of vertical component of motion for surface receivers between x = −500 and x = 500 at surface of the hill.

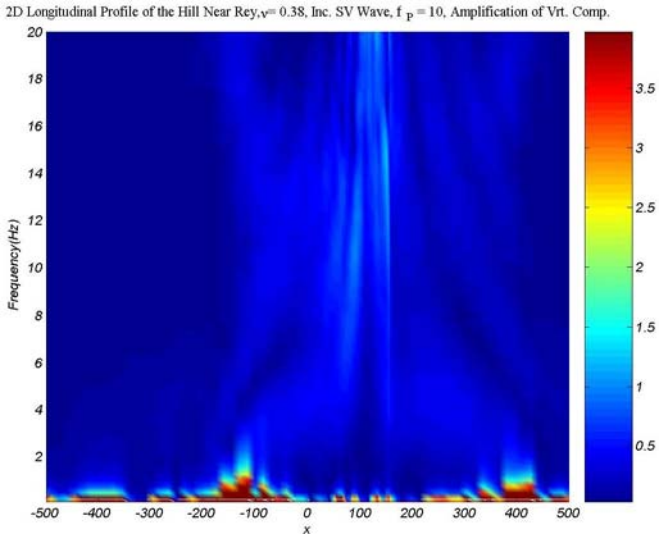

Fig. 15. Incidence of a vertically propagating SV wave (freq. 10Hz). Amplification pattern of vertical component of motion for surface receivers between x = −500 and x = 500 at surface of the hill.

TRANSVERSE PROFILE

As in the previous part, the hill has been instrumented in two directions. Hence, the hill was modeled in a way that the two instrumented profile subjected to SV waves, could be analyzied. The layout of the model has been shown in fig. 16. It consists of 445 nodes and 222 quadratic boundary elements at the boundary and 319 enclosing elements. The material properties have been defined in table 1. The pattern of amplification is very similar to that of longitudinal model which has not been shown here.

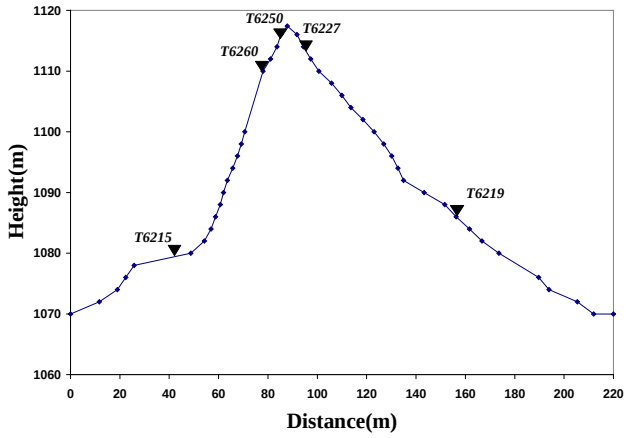

Fig. 16. Incidence of a vertically propagating SV wave (freq. 6-10Hz). Amplification of the crest of the hill (longitudinal profile).

Regarding the horizontal component of the motion, if the incident wave possesses a long or very long wavelength as it is

shown in fig. 17, the maximum amplification factor occurs at the top of the hill and the amplification curve decays towards the bases.

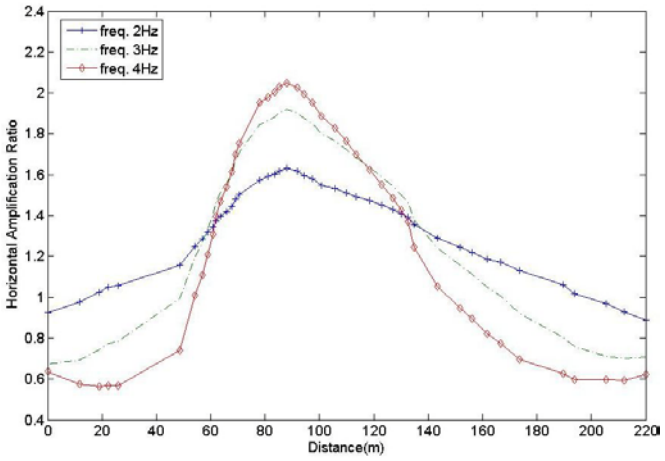

Fig. 17. Amplification curves of the hill in the case of incidence of a vertically propagating SV wave (freq. 2-4Hz).

In the case of an incident wave with a medium wavelength, although the same behavior would be seen, some de-amplification would also occur at the bases, as it is shown in fig 18.

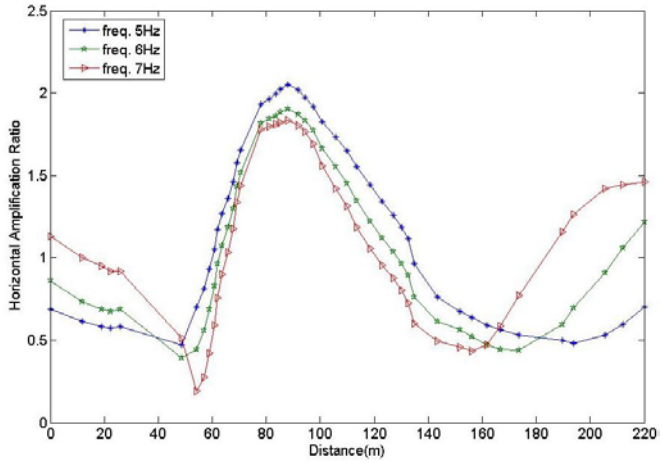

Fig. 18. Amplification curves of the hill in the case of incidence of a vertically propagating SV wave (freq. 5-7Hz).

In an incident wave with a short or very short wavelength, the number of deamplification zones along the hill would increase. The amplification curves of the hill may experience their maximum at points other than the crest (fig. 19).

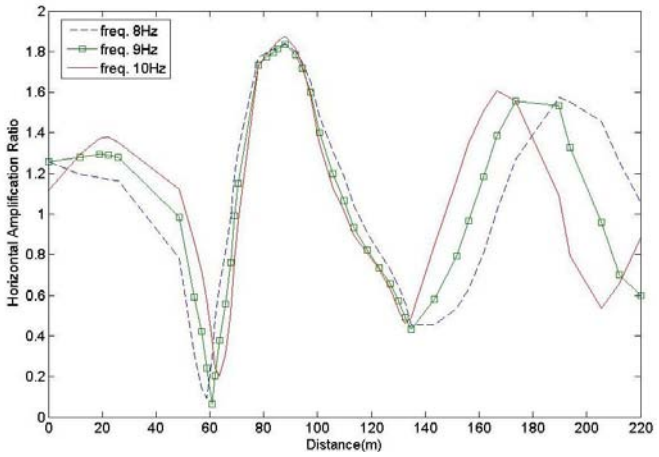

Fig. 19. Amplification curves of the hill in the case of incidence of a vertically propagating SV wave (freq. 8-10Hz).

HORIZONTAL TO HORIZONTAL SPECTRAL RATIO

To verify the hypothesis proposed for frequency of 1.3 Hz and as the site is relatively small scale irregularity, some horizontal to horizontal spectral ratios for different stations on the hill with respect to stations on the base has been fulfilled. Some of the results have been shown in the fig. 20 and 21 .

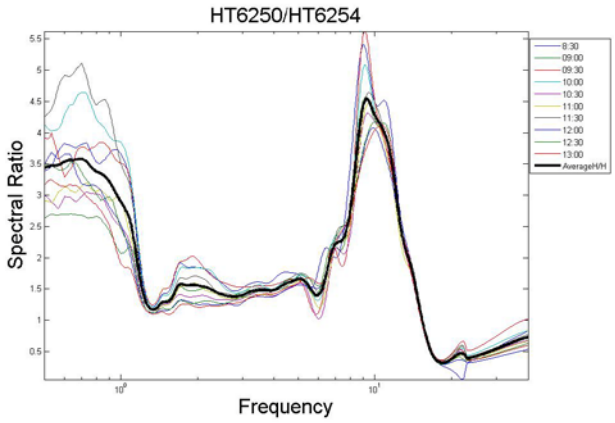

Fig. 20. The horizontal to horizontal spectral ratio for station T6250 along the slope to the base station T6254 (longitudunal profile).

As it is obviously could be seen, the curves around the frequency of 1.3 Hz shows an amplitude around one which verified the hypothesis that in all stations an industrial noise affect the stations. On the other hand, around other frequencies like 10 Hz, depending on the situation of the seismic station, it shows different amplification. Of course, it seems to be not that much accurate quantitatively, but qualitatively it is quite similar to what it would be expected. Besides, as it is excpected the spectral ratio of the station on the top of the hill is greater than the spectral ratio of the station along the hill.

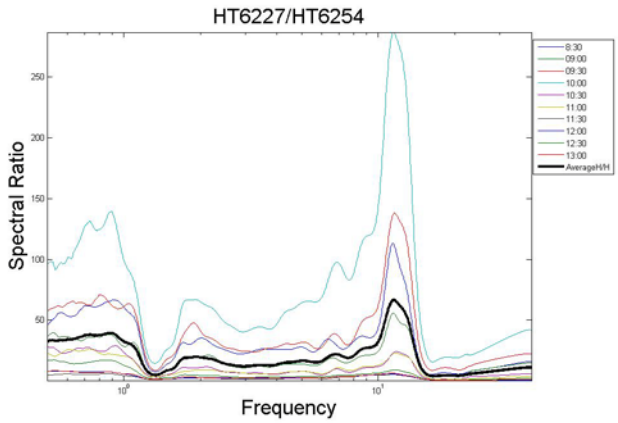

Fig. 21. The horizontal to horizontal spectral ratio for top station T6227 to the base station T6254 (longitudunal profile).

The same results could be seen along the transverse profile which has not been shown here.

CONCLUDING REMARKS

The observed amplification in experimental studies, can be observed for the frequencies around 10 Hz specially on transverse section. This frequency correspond to a trough on H/V curves for stations installed at the base of the hill, so it could be attributed to the topographic effect. The are no similarity between this result and the result of numerical modeling.. These discrepancies may be related to the following results;

1- Existence of industrial noise near to the site, may be one of the results of differences.
2- The incapability of H/V technique for distinguishing thefundamental frequency of topographic irregularity.
3- The differences of the wave-fields using in in the numerical modeling, and microtrmors. In the first one the body waves like SV has been used while the microtremors consisted predominantly of surface waves.

ACKNOWLEDGMENTS

The authors acknowledge IIEES staffs in seismology laboratory for their kind help in installing seismic stations.

REFERENCES

Ashford, A., Sitar, N. [1997]. "Analysis of Topographic Amplification of Inclined Shear Waves in a Steep Coastal Bluff", BSSA, Vol. 87, No. 3, pp. 792-700.

Athanasopoulos, G.A., Pelekis, P.C., Leonidou, E.A. [1999]. "Effects of surface topography on seismic ground response in the Egion (Greece) 15 June 1995 earthquake", Soil Dyn. and Earthquake Engrg., Vol. 18, No. 2, pp. 135-149.

Celebi, B. [1987]. "Topographical and Geological Amplification Determined From Strong Ground Motion And AfterShock Records of the 3 March 1985 Chile Earhquake", BSSA, Vol. 77, No. 1, pp. 1147-1167.

Celebi, B. [1991]. "Topographical and Geological Amplification:Case Studies and Engineering Implications", Structural Safety, Vol. 10, No. 1, pp. 199-217.

Davoodi M., Amel Sakhi M., Jafari M. K., 2008. "Using New Signal Processing Techniques in Analyzing Masjed Soleyman Embankment Dam's Explosion Records", The 6th International Conference on Case Histories in Geotechnical Engineering, August 11-16, 2008, USA.

Haghshenas, A. [2005]. "*Condition Géotechniques et Aléa Sismique Local à Téhéran*", Ph.D Thesis, Joseph Fourier University, Grenoble, France.

Jafari, M.K., Davoodi, M. [2006]. "Dynamic Characteristic Evaluation of Masjed Soleiman Dam Using Insitu Dynamic Tests" Canadian Geotech. J., Vol. 43, pp. 997-1014.

Kamalian, M., Jafari, M., Sohrabi-Bidar, A.,Razmakhah, A. [2007]. "Seismic response of 2-D semi-sine shaped hills to vertically propagating incident waves: amplification patterns and engineering applications" Earthquake Spectra. Vol. 24, No. 2, pp. 997-1014.

Nakamura, Y. [1989]. "A Method for dynamic characteristic Estimation of Subsurface using Microtremor on the Ground Surface" RTRI. Vol. 30, No. 1.